Catalysis Letters 28 (1994) 99–108

Characterization of fresh and lined-out bulk FeMo sulfide catalysts

J.Y. Koo and T.C. Ho [1]

Corporate Research Laboratories, Exxon Research and Engineering Company,
Annandale, NJ 08801, USA

Received 18 March 1994; accepted 11 June 1994

As reported previously, while a hydrodenitrogenation-selective FeMo sulfide catalyst maintained its activity in a 600 h accelerated aging test, the catalyst lost its hydrodenitrogenation activity fairly rapidly during the early stages of the test. This study is aimed at identifying the origin of the initial activity loss. Characterization of fresh and lined-out catalysts has indicated that the initial activity decline appears to be caused by decomposition of a single-phase amorphous FeMo sulfide.

Keywords: catalyst deactivation; FeMo sulfide; hydrotreating catalysts; scanning transmission electron microscope; energy dispersive microanalysis; microdiffraction

1. Introduction

As shown previously [1,2], a bulk (unsupported) FeMo sulfide was found to have a high selectivity toward hydrodenitrogenation (HDN) relative to hydrodesulfurization (HDS). Its HDN and HDS activities can be significantly enhanced through copromotion with Co or Ni [3]. Results from a 600 h accelerated aging test indicated that this bulk catalyst is thermally stable [1].

However, a fairly rapid loss in the HDN activity was noted when the catalyst was placed on stream. The purpose of this study was to understand the cause of this initial activity loss. The fresh and lined-out catalysts were characterized using a high-resolution scanning transmission electron microscope (STEM) coupled with energy dispersive microanalysis and microdiffraction.

2. Experimental

2.1. CATALYST

The bulk FeMo sulfide catalyst used in this study was prepared in the same manner as that described in ref. [1]. Basically, the catalyst was prepared from thermal

---

[1] To whom correspondence should be addressed.

decomposition of iron bis(diethylenetriamine) thiomolybdate [4] at 325°C for 3 h with a 10% H_2S-in-H_2 mixture. Ref. [1] may be referred to for details.

2.2. FEEDSTOCK

A light catalytic cycle oil, a highly aromatic stock, was used throughout the present study. The properties of this feedstock can be found in ref. [1].

2.3. EQUIPMENT AND PROCEDURE

The evaluation experiments were conducted in an automated trickle-bed reactor equipped with a calibrated feed burette, pump, gas–liquid separator, and product liquid collector. The reactor was a 3/8 inch 316 stainless steel pipe, which was packed with 20 cm^3 of catalyst (20/40 mesh granules) in the central zone and 1/16″ alundum in the fore and after zones. The attainment of isothermal conditions was indicated by temperature measurement across the bed. Reaction conditions were: temperature, 325°C; pressure, 3.15 MPa; hydrogen treat gas, 3000 SCF/B (standard cubic feet/barrel); and liquid hourly space velocity (LHSV), 4.0. Again, ref. [1] may be referred to for details.

2.4. ELEMENTAL ANALYSIS

After purging with N_2, the liquid product was analyzed for total sulfur by X-ray fluorescence using external standards. This was done with a Princeton Gamma-Tech model 100 chemical analyzer which contains a ^{55}Fe radioactive source. The total nitrogen was analyzed by combustion and chemiluminescence using the Antek analyzer.

2.5. ELECTRON MICROSCOPY

The morphology and crystal structure determinations of the constituent phases were carried out using high resolution and analytical electron microscopy. In this procedure [5] the transition metal sulfide powder was prepared for the transmission electron microscope (TEM) by crushing in an agate mortar and pestle to produce powder fragments through which an electron beam could pass. The crushed powder was ultrasonically dispersed in hexane and a drop of this suspension was allowed to dry onto a standard 3 mm TEM grid, which was covered with a thin ($\leqslant$200 Å) amorphous carbon film. Samples were analyzed in a Philips 400T FEG STEM at 100 kV by bright field imaging, energy dispersive X-ray microanalysis, and microdiffraction.

Quantitative chemical analysis was obtained by the thin foil ratio method [6], and the absorption effects were analyzed and corrected using the procedure described by Goldstein [7]. X-ray fluorescence spectra were generated from the excited volume of the sample defined by the cylinder of 100 Å probe size and the thickness of the sample (typically ~ 1000 Å).

3. Results and discussion

3.1. ACTIVITY LOSS

Shown in fig. 1 are the HDN *initial* life data on the FeMo catalyst. The corresponding HDS data are shown in fig. 2. The data are corrected for fluctuations in LHSV according to the previously determined kinetics for HDN and HDS [1]. As can be seen from fig. 1, the rate of initial activity decline can be characterized by a time constant on the order of 100 h. In contrast, the HDS data remained virtually flat, suggesting that the nature of catalytic sites for HDN and HDS are *not* entirely the same. It is not our intent here to discuss the differences between HDN and HDS sites.

3.2. MICROSTRUCTURE

Transmission electron micrographs for the fresh and lined-out catalysts are shown in figs. 3, 4, 7 and 8. Both catalysts contained a small quantity (<5%) of relatively large (0.1–1 μm in size) $Fe_{1-x}S$ crystalline particles. A typical particle is shown in fig. 3. The size, morphology, and volume fraction of these large particles are similar in both fresh and lined-out catalysts, which suggests that the particles have no significant influence on activity or deactivation.

The fresh catalyst exhibits two distinct morphologies as shown in figs. 4A and 4B. Fig. 4A shows the dominant phase found in the fresh catalyst. This phase is basically *amorphous* in nature with occasional appearance of single or double lines

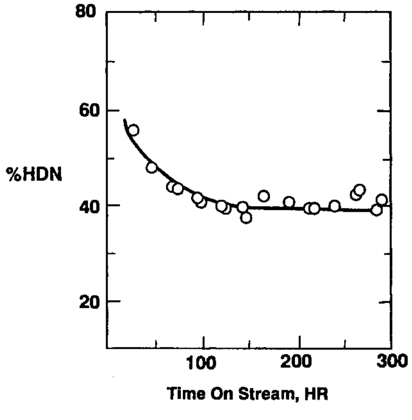

Fig. 1. Percent HDN as a function of on-stream time (h); feedstock: light catalytic cycle oil; conditions: 325°C, 3.15 MPa, 4.0 LHSV, 3000 SCF H_2/barrel oil.

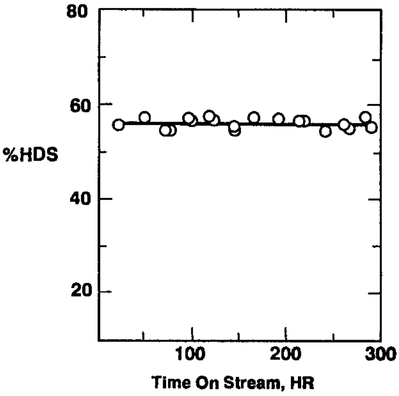

Fig. 2. Percent HDS as a function of on-stream time (h); feedstock: light catalytic cycle oil; conditions: 325°C, 3.15 MPa, 4.0 LHSV, 3000 SCF H_2/barrel oil.

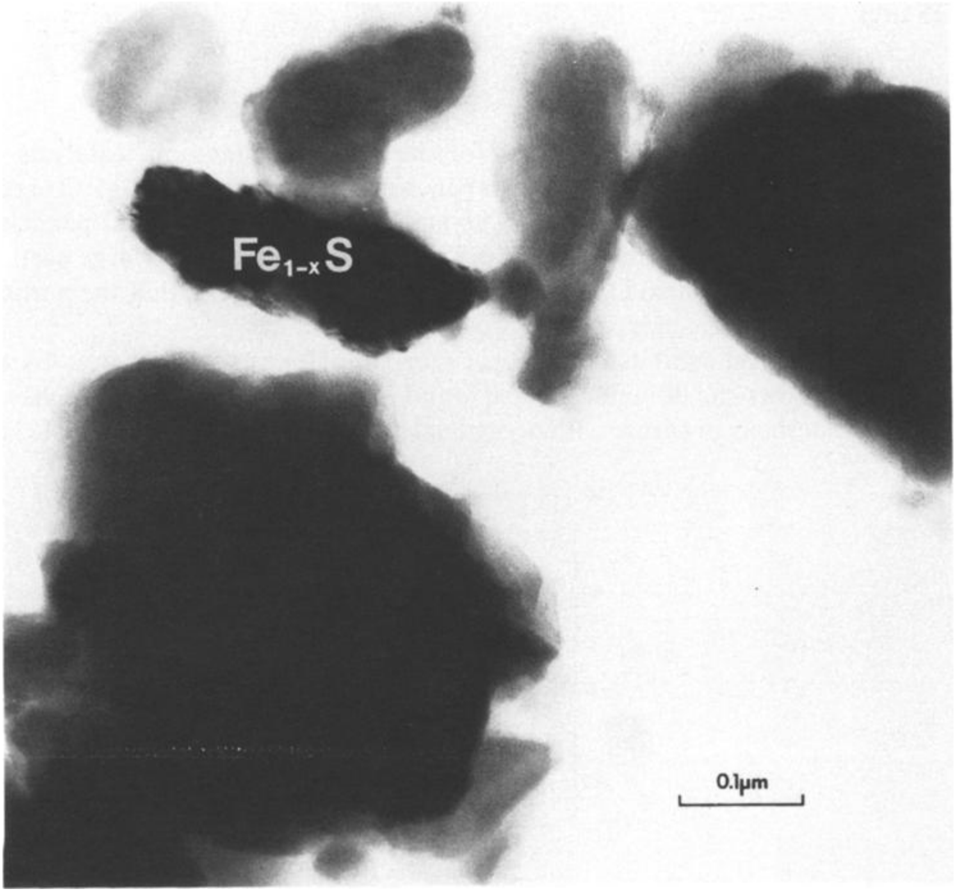

Fig. 3. Transmission electron micrograph of fresh catalyst showing a large $Fe_{1-x}S$ crystallite. The rest of the particles shown in the image is the amorphous Fe–Mo–S phase (see fig. 4A).

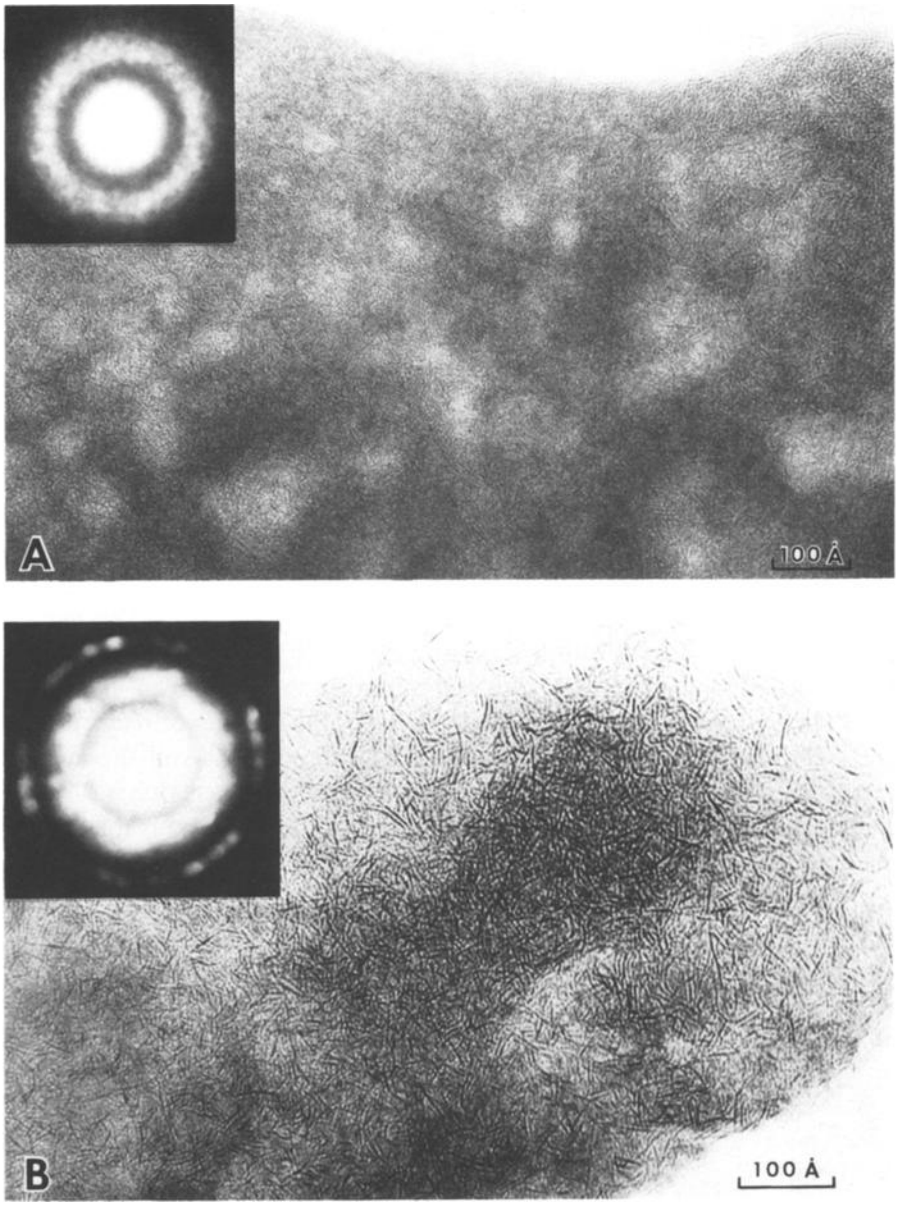

Fig. 4. Transmission electron micrograph of fresh catalyst showing (A) predominantly amorphous phase, which is a major phase, and (B) single and double layer MoS_2-like structure, which is a minor phase.

with about 6.2 Å in spacing. The amorphous nature is also observed in the corresponding microdiffraction pattern (inset) where a broad ring indicates the characteristic amorphous structure. It can also be noted from the diffraction pattern that the ring intensity is not uniformly smooth, but rather somewhat spotty. This result is consistent with the presence of very short single or double lines observed in the image.

Another type of morphology found in the fresh catalyst is illustrated in fig. 4B, which shows predominantly single or double layer MoS_2-like structures. The layer spacing is measured to be about 6.2 Å. The corresponding microdiffraction pattern (inset) obtained from a 100 Å probe size reveals both the MoS_2-like crystalline spots and the amorphous diffraction ring. The crystalline diffraction spots are quite diffuse in intensity, suggesting that the phase is poorly crystalline in nature and lacks long-range periodicity in atomic arrangement. This observation is also consistent with the findings in the image (fig. 4B). X-ray elemental analysis using a 100 Å probe size indicated that the fresh catalyst is chemically homogeneous within the 100 Å spatial resolution. The results of the compositional analysis are summarized in the ternary composition diagram, fig. 5. It is noted that the Fe/Mo atomic ratio is one to one. Large $Fe_{1-x}S$ crystallites, as shown in fig. 3, are not included in this composition plot.

While the fresh catalyst is chemically homogeneous and predominantly amorphous, the lined-out catalyst showed a clear evidence of phase separation and chemical inhomogeneity, as can be seen from the composition plot shown in fig. 6. Here the large $Fe_{1-x}S$ crystallites shown in fig. 3 are not included in the analysis. The corresponding transmission electron micrographs are shown in figs. 7 and 8. Analysis showed that at low magnification, fig. 7, the patches of black areas represent relatively small iron sulfide crystallites (100–300 Å). And the surrounding layered phase is an Fe-containing, MoS_2-like crystalline phase rich in Mo. Some of the iron sulfide crystallites are not visible as black patches in this micrograph due to the orientation of the sample. It should also be emphasized that the above phase

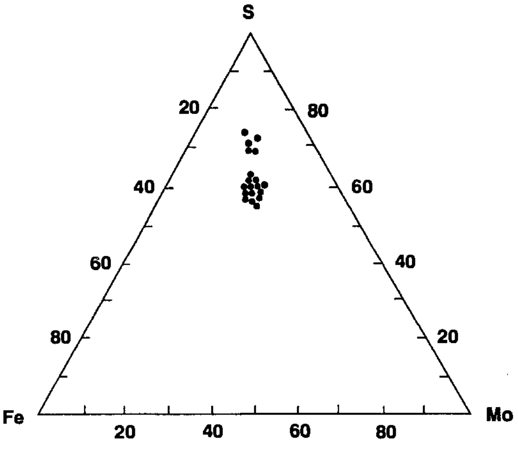

Fig. 5. Ternary composition diagram for fresh catalyst.

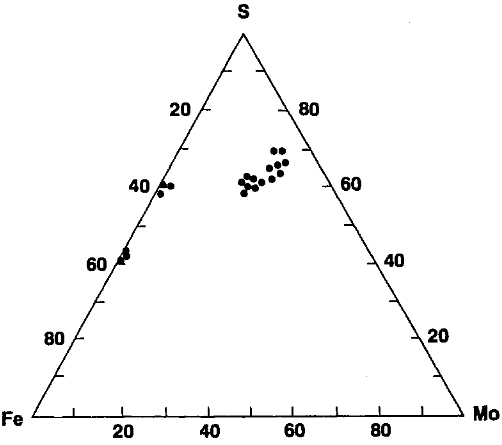

Fig. 6. Ternary composition diagram for lined-out catalyst.

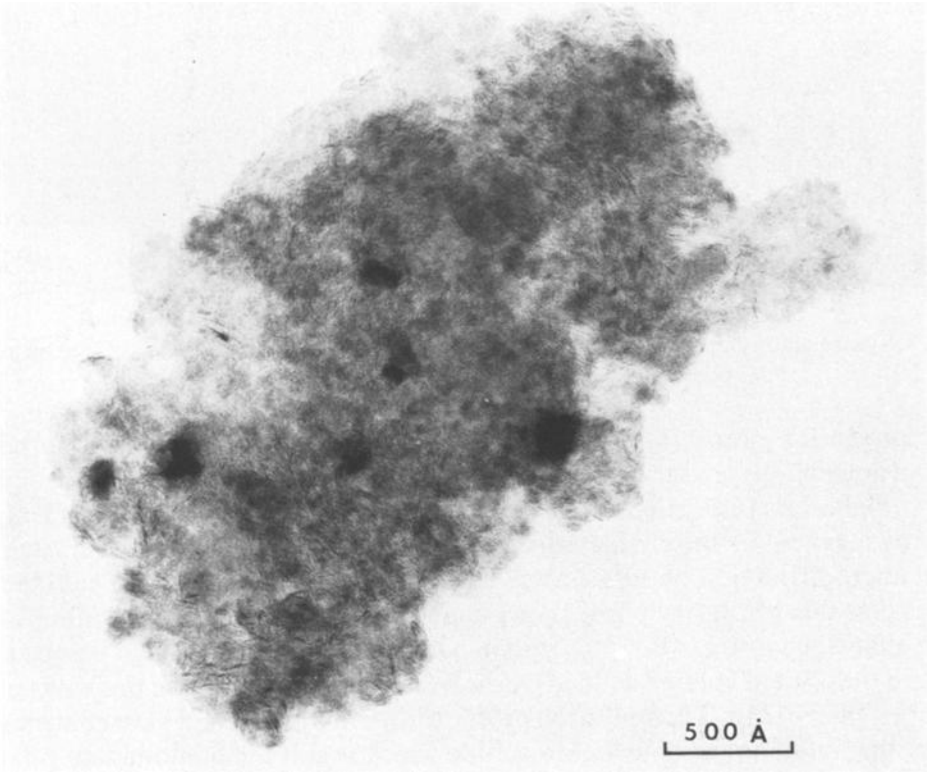

Fig. 7. Transmission electron micrograph of lined-out catalyst revealing localized phase decomposition products. Black patches are small crystalline iron sulfide particles and the multi-layered structure is an MoS_2-like phase. A significant amount of amorphous phase is still retained.

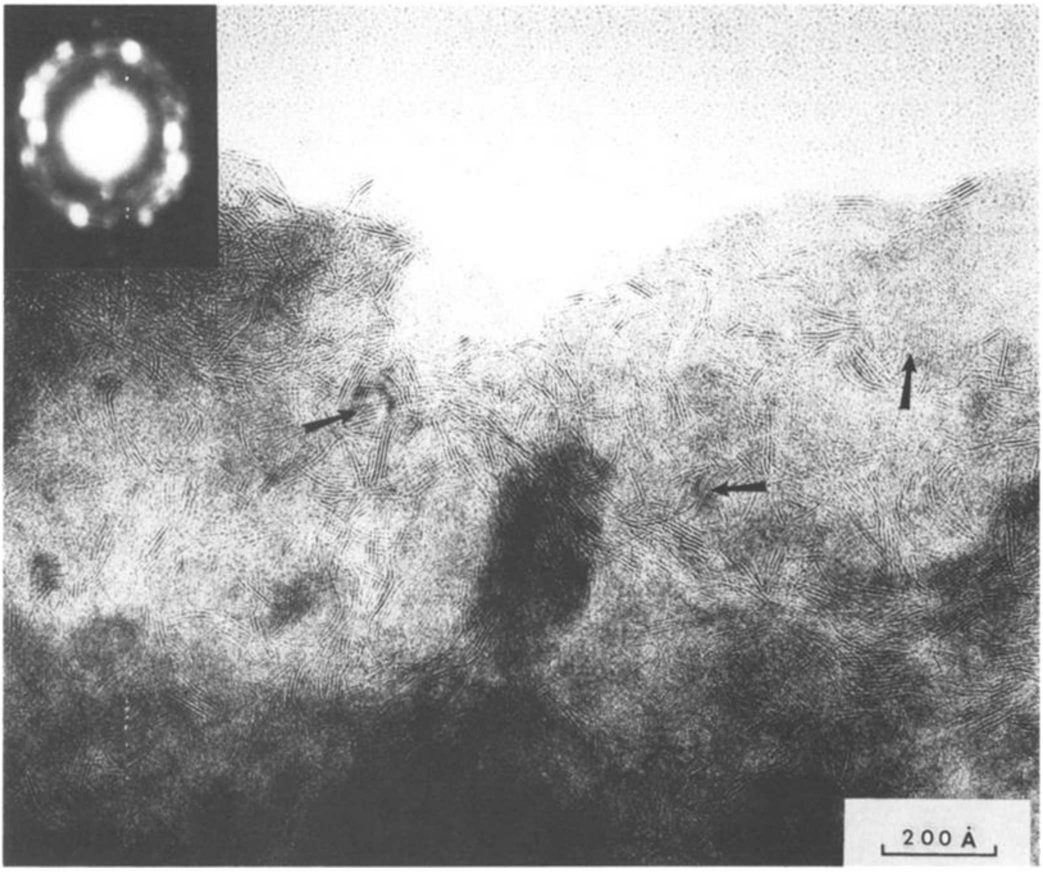

Fig. 8. Transmission electron micrograph of lined-out catalyst showing the details of the constituent phases. Arrows indicate some of the $Fe_{1-x}S$ crystallites.

decomposition occurs only *locally*; there remains a significant fraction of the initial amorphous phase which has not undergone phase decomposition.

At higher magnification, fig. 8, small $Fe_{1-x}S$ crystallites are clearly identified (arrow marked) by the characteristic lattice fringes present inside the crystallites. The microdiffraction pattern (inset) taken from the Mo-rich FeMo sulfide indicates that this MoS_2-like phase shows a much more well-defined crystalline structure than that in fig. 4B. Since microanalysis provides an average composition within the excited volume defined by the 100 Å probe size and the thickness of the sample, the Fe–Mo–S composition profile shown in fig. 6 should have contribution from the initial amorphous FeMo sulfide which is still the predominant phase in the lined-out catalyst. Comparing the composition diagram of the fresh catalyst (fig. 5) with that of the lined-out catalyst (fig. 6), one can see a trend of phase decomposition occurring during the lining-out period in the activity test.

The above results indicate that the predominant single phase, amorphous

FeMo sulfide is the active species most likely responsible for the observed high HDN selectivity. This result is consistent with that of Mössbauer studies [1]. While on oil, this phase, as driven by thermodynamics, slowly becomes converted into two separate phases consisting of small iron sulfide particles and the surrounding MoS_2-like phase. The rate of this conversion becomes progressively slower as the conversion proceeds. This is probably because iron sulfide is gradually encapsulated by the MoS_2-like phase which inhibits further growth of iron sulfide. In other words, the "stripping" of iron from the initial amorphous FeMo sulfide becomes increasingly difficult due to the growing diffusion barrier resulting from the encapsulation. Larger iron sulfide crystallite, on the other hand, can form the growth of iron sulfide near the exterior part of the sample.

The term "amorphous" used here can include a single or double layer of MoS_2 which has very short length up to about 10 Å. This is due to the fact that the bright field image of such tiny crystalline units cannot be readily distinguished from the phase contrast image of a truly amorphous material. In fact, there is some evidence from fig. 4A that an extremely small crystalline MoS_2 phase is present in the fresh FeMo sulfide catalyst. The amorphous phase contains equal amounts of Fe and Mo within the 100 Å spatial resolution. The specific atomic arrangement of Fe, Mo, and S in the amorphous structure is unknown at present. However, iron seems to thermally stabilize the amorphous phase and thus slows down thermal decomposition of the phase into two separate phases.

4. Conclusions

(1) Fresh catalyst consists predominantly of a single phase, amorphous FeMo sulfide phase which appears to be the active species responsible for the high HDN selectivity. The Fe/Mo atomic ratio in this phase is near unity.

(2) While on oil, the amorphous phase partially becomes converted to two separate phases consisting of iron sulfide crystalline particles and an MoS_2-like phase. HDN activity decreases as the phase separation proceeds. The MoS_2-like phase surrounds the iron sulfide particle as this particle grows and appears to inhibit further growth of the iron sulfide crystallites. This phenomenon may explain why a final steady state activity was observed in the long-term life test reported previously [1].

(3) A higher HDN activity and selectivity throughout the life of the catalyst may be attained if the initial amorphous FeMo sulfide phase can be stabilized.

References

[1] T.C. Ho, A.J. Jacobson, R.R. Chianelli and C.R.F. Lund, J. Catal. 138 (1992) 351.
[2] T.C. Ho, Ind. Eng. Res. 32 (1993) 1568.

[3] T.C. Ho, R.R. Chianelli and A.J. Jacobson, Appl. Catal., in press.
[4] T.C. Ho, A.R. Young, A.J. Jacobson and R.R. Chianelli, US Patent 4 591 429 (1986).
[5] P.C. Flynn, S.E. Wanke and P.S. Turner, J. Catal. 33 (1974) 233.
[6] G. Cliff and G.W. Lovimer, Microscopy 103 (1975) 203.
[7] J.I. Goldstein, in: *Introduction to Analytical Electron Microscopy*, eds. J.J. Hren, J.I. Goldstein and D.C. Joy (Plenum Press, New York, 1979) pp. 83-120.